

Article

# Chemical Characteristics and Sources of Submicron Particles in a City with Heavy Pollution in China

Jianlei Lang , Shengyue Li, Shuiyuan Cheng, Ying Zhou, Dongsheng Chen, Yanyun Zhang, Hanyu Zhang and Haiyan Wang

Key Laboratory of Beijing on Regional Air Pollution Control, College of Environmental & Energy Engineering, Beijing University of Technology, Beijing 100124, China; lishengyue@emails.bjut.edu.cn (S.L.); chengsy@bjut.edu.cn (S.C.); y.zhou@bjut.edu.cn (Yi.Z.); dschen@bjut.edu.cn (D.C.); 13641375542@163.com (Ya.Z.); zhy2016@emails.bjut.edu.cn (H.Z.); why@bjut.edu.cn (H.W.)

\* Correspondence: jllang@bjut.edu.cn; Tel.: +86-10-6739-6628

Received: 7 August 2018; Accepted: 1 October 2018; Published: 5 October 2018



**Abstract:** Submicron particle (PM<sub>1</sub>) pollution has received increased attention in recent years; however, few studies have focused on such pollution in the city of Shijiazhuang (SJZ), which is one of the most polluted cities in the world. In this study, we conducted an intensive simultaneous sampling of PM<sub>1</sub> and PM<sub>2.5</sub> in autumn 2016, in order to explore pollution characteristics and sources in SJZ. The results showed that the average mass concentrations of PM<sub>1</sub> and PM<sub>2.5</sub> were 70.51 µg/m<sup>3</sup> and 91.68 µg/m<sup>3</sup>, respectively, and the average ratio of PM<sub>1</sub>/PM<sub>2.5</sub> was 0.75. Secondary inorganic aerosol (SIA) was the dominant component in PM<sub>1</sub> (35.9%) and PM<sub>2.5</sub> (32.3%). An analysis of haze episodes found that SIA had a significant influence on PM<sub>1</sub> pollution, NH<sub>4</sub><sup>+</sup> promoted the formation of pollution, and SO<sub>4</sub><sup>2-</sup> and NO<sub>3</sub><sup>-</sup> presented different chemical mechanisms. Additionally, the results of source apportionment implied that secondary source, biomass burning and coal combustion, traffic, industry, and dust were the major pollution sources for SJZ, accounting for 45.4%, 18.9%, 15.7%, 10.3%, and 9.8% of PM<sub>1</sub>, respectively, and for 42.4%, 18.8%, 12.2%, 10.2%, and 16.4% of PM<sub>2.5</sub>, respectively. Southern Hebei, mid-eastern Shanxi, and northern Henan were the major contribution regions during the study period. Three transport pathways of pollutants were put forward, including airflows from Shanxi with secondary source, airflows from the central Beijing–Tianjin–Hebei region with fossil fuel burning source, and airflows from the southern North China Plain with biomass burning source. The systematic analysis of PM<sub>1</sub> could provide scientific support for the creation of an air pollution mitigation policy in SJZ and similar regions.

**Keywords:** PM<sub>1</sub>; PM<sub>2.5</sub>; chemical characteristics; source apportionment; haze pollution; Shijiazhuang

## 1. Introduction

With the rapid development of the economy and acceleration of urbanization, fine particulate matter pollution is gradually attracting attention in China [1–5]. Issues related to submicron particles (PM<sub>1</sub>, particles with aerodynamic diameters less than or equal to 1 µm) have become more severe in recent years. According to previous studies, PM<sub>1</sub> has been characterized by high mass concentration and high proportion in PM<sub>2.5</sub> [6–8], and some major components were more distributed in PM<sub>1</sub> than in PM<sub>1–2.5</sub> (e.g., NH<sub>4</sub><sup>+</sup>, SO<sub>4</sub><sup>2-</sup>, and K<sup>+</sup>), which played prominent roles in haze episode formation in China [8,9]. As a result, PM<sub>1</sub> has had a serious impact on air quality, especially for heavy pollutions. Additionally, significant health risks of PM<sub>1</sub> were also found in different ways, such as respiratory symptoms, carcinogenic effect, and endocrine [10–14]. Consequently, the mitigation of PM<sub>1</sub> pollution deserves special attention. Before that, the chemical characteristics and sources of PM<sub>1</sub> should be investigated, in order to provide scientific support for policy making.

Some studies have concentrated on only one or several components of PM<sub>1</sub>, such as elemental composition [15], black carbon (BC) [16], organic carbon (OC) and elemental carbon (EC) [17,18], and water-soluble inorganic ions [19]. Most studies have preferred to explore the characteristics of dominant compositions (e.g., NO<sub>3</sub><sup>-</sup>, SO<sub>4</sub><sup>2-</sup>, NH<sub>4</sub><sup>+</sup>, Cl<sup>-</sup>, OC, and BC) based on online monitoring, such as chemical profiles [20,21], temporal variations [22], pollution sources identified by positive matrix factorization (PMF) or principal component analysis (PCA) models [9,23], and regional contribution resolved by the Hybrid Single Particle Lagrangian Integrated Trajectory (HYSPLIT) model [24]. Only limited studies have carried out analyses based on a relatively complete spectrum of species from offline sampling [25,26]. Incomplete spectra of species limit the comprehensive understanding of chemical characteristics (including components of carbonaceous matter, ions, and elements) and the identification of the overall pollution sources. For example, K<sup>+</sup> and typical elements (e.g., Fe, Pb, and Ni) cannot be detected by the most commonly used PM<sub>1</sub> monitoring instrument—the ACSM (Aerosol Chemical Speciation Monitor) [17,21,23]—however, these species are the key tracers for the identification of biomass burning, and industrial and traffic sources. All in all, more detailed data regarding PM<sub>1</sub> species is urgently needed, as they are essential to obtaining a better knowledge of submicron particulate pollution in terms of chemical characteristics and source contributions.

Alarming, although Shijiazhuang (SJZ) is one of the most polluted cities in China, few studies on PM<sub>1</sub> have been conducted there, and the relevant chemical characteristics and pollution sources remain ambiguous. As the provincial capital of Hebei province, SJZ has been suffering from heavy haze pollution for a long time. The air quality of this city has consistently been ranked as the third worst nationwide in recent years, and finally dropped to last place in 2017 as of the newest statistics [27]. Despite years of emission control, there were still 71 heavily polluted days (daily PM<sub>2.5</sub> concentration >150 µg/m<sup>3</sup>) in SJZ in 2016, with an annual average PM<sub>2.5</sub> concentration of 99 µg/m<sup>3</sup> [28], significantly exceeding the Chinese National Ambient Air Quality Standards (CNAAQS) for annual mean PM<sub>2.5</sub> concentration (35 µg/m<sup>3</sup>). Furthermore, because of the high emissions and poor air quality, regional transport effects [29] and health problems [30] were also serious and intractable in this city. Therefore, making clear PM<sub>1</sub> features in this heavily polluted city is probably important as a reference for pollution control in other similar regions worldwide.

Seasonal-scale analysis is a prevalent method for the study of aerosols due to the constraints of time and energy. Autumn is a season when heavy air pollution frequently occurs in China [31]. In this season, the representative pollution source, biomass burning, is noteworthy for its large emissions [32] and multifaceted effects [33]. Hence, in this study, an intensive campaign to sample PM<sub>1</sub> and PM<sub>2.5</sub> was conducted in autumn 2016 in SJZ. Detailed chemical species were further analyzed, including trace elements (TE), ions, OC, and EC. The characteristics of PM<sub>1</sub> and PM<sub>2.5</sub> at different levels of pollution, the sectoral and regional sources, and the transport pathways of pollutants in SJZ were then investigated. The purpose of this case study is to provide new knowledge about the characteristics of PM<sub>1</sub> from multiple aspects in the area with heavy industry and severe haze pollutions, supporting the improvement of air quality and the establishment of emission control measures.

## 2. Experiments and Methodology

### 2.1. City Description

The city of SJZ is the provincial capital of Hebei province, with a permanent population of 10.78 million people in 2016 [34]. The industrial structure of SJZ is dominated by secondary industry (45.0%) and tertiary industry (46.8%). It is an important base of agricultural products and grain in China, such as oil plants, wheat, and cotton, providing a yield of 1.90 million tons, 2.57 million tons, and 7.70 thousand tons, respectively, in 2015 [35]. The primary industrial types include steel; metallurgy; equipment manufacturing; petrochemical; architectural material; food; and, especially, the pharmaceutical and textile industries, which occupy a vital position nationwide [34]. However, because of its coal-based, high energy consumption industrial structure, SJZ has been suffering from

heavy haze pollution in recent years (Figure 1a). SJZ is located in the east of China, west of the North China Plain (NCP), southwest of the Beijing–Tianjin–Hebei (BTH) region and west of the Taihang Mountains, adjacent to two heavy industry cities (Xingtai and Hengshui) in the south and east (Figure 1b); the special geography and terrain probably cause the distinct polluted characteristics and transport pathway of SJZ.

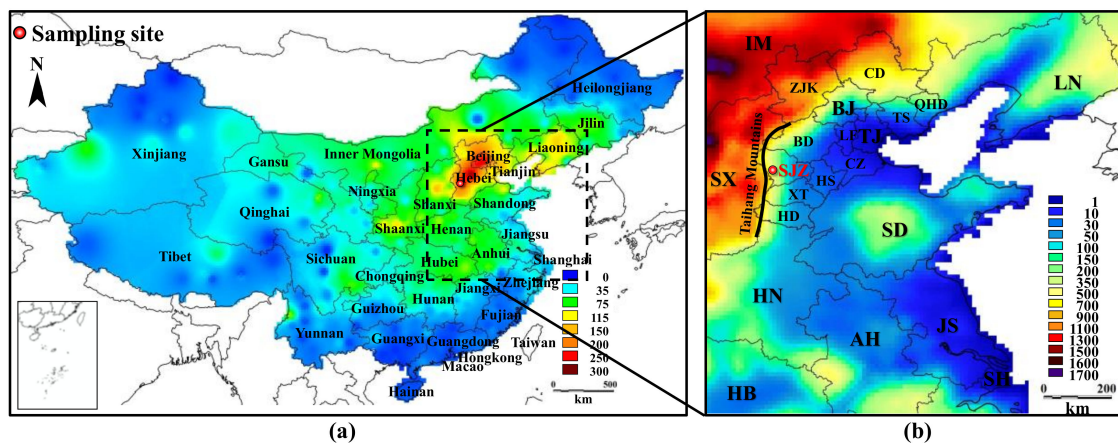


**Figure 1.** The location of the sampling site in SJZ. (a) The spatial variations of PM<sub>2.5</sub> concentration ( $\mu\text{g}/\text{m}^3$ ) in China during the monitoring period; (b) the elevation (m) distribution of the North China Plain (CD: Chengde; ZJK: Zhangjiakou; QHD: Qinhuangdao; TS: Tangshan; LF: Langfang; BD: Baoding; CZ: Cangzhou; HS: Hengshui; SJZ: Shijiazhuang; XT: Xingtai; HD: Handan).

## 2.2. Sampling Program

Daily 24 h (09:00 to 09:00 the next day) measurements of PM<sub>1</sub> and PM<sub>2.5</sub> were intensively performed between 8 October and 1 November 2016. The monitoring period was mainly in October, thus avoiding the influence of late summer and the heating season (which begins around 15 November [36]). The monitoring period involved at least three pollution process variations, as one process generally lasts three to seven days [37,38], and could basically represent the common condition in autumn. The sampling site is located in the SJZ Environmental Monitoring Center ( $38.02^\circ$  N,  $114.53^\circ$  E) on the roof of a five-floor building ( $\sim 16$  m in height). It is surrounded by residential and commercial areas, next to roads with moderate traffic, and could basically represent the urban condition.

Samples of PM were collected with two URG systems (URG, Chapel Hill, NC, USA), one with cutoff in aerodynamic diameter at  $1 \mu\text{m}$  (PM<sub>1</sub>) and the other at  $2.5 \mu\text{m}$  (PM<sub>2.5</sub>), with a flow rate of 16.7 L/min. The sampling membrane included Whatmans 41 filters (Whatman Inc., Maidstone, UK) and quartz fiber filters (Whatman Inc., Maidstone, UK), which were used for the analysis of elements and ions, and OC and EC, respectively. After sampling, the filters were conserved in polyethylene plastic bags and stored in a refrigerator. The samples were finally equilibrated for 48 h and weighed at a temperature of  $20 \pm 5^\circ\text{C}$  and relative humidity of  $40 \pm 2\%$ . The weight of the filters was determined using an electronic balance (Sartorius TB-215D) before and after sampling, with a precision of 0.01 mg. Multiple weighing steps (three or more times) were performed until the absolute deviation was less than or equal to 0.03 mg. The whole program had strict quality control to avoid sample contamination. Additionally, conventional meteorological parameters around the sampling site were synchronously monitored, including temperature, wind direction, wind speed, relative humidity, and air pressure.

## 2.3. Chemical Analysis

A total of 50 samples were collected, and 26 species were analyzed, including Na, Mg, Al, S, Ca, Ti, Cr, Mn, Fe, Ni, Cu, Zn, Sr, Pb, Na<sup>+</sup>, K<sup>+</sup>, NH<sub>4</sub><sup>+</sup>, Ca<sup>2+</sup>, Mg<sup>2+</sup>, F<sup>-</sup>, Cl<sup>-</sup>, NO<sub>2</sub><sup>-</sup>, NO<sub>3</sub><sup>-</sup>, SO<sub>4</sub><sup>2-</sup>, OC, and EC. A total of 14 metallic elements were measured by inductively coupled plasma mass spectrometry (ICP-MS; 7500a, Thermo), and S was determined by inductively coupled plasma atomic emission

spectroscopy (ICP-AES). The samples were pre-treated by the closed vessel digestion method before elemental analysis, and the relative standard deviations (RSD) were generally below 5%. For ion analysis, the ion chromatograph (IC; Metrohm 861 Advanced Compact IC) was applied, with detection limits of less than 0.04 mg/L for anions and 0.006 mg/L for cations. The RSD of each ion was less than 5%. OC and EC in PM were analyzed by the optical carbon analyzer model (DRL Model 2001A, Desert research institute, Reno, NV, USA). The detection limits of total organic carbon and total elemental carbon were 0.82  $\mu\text{g C}/\text{cm}^3$  and 0.20  $\mu\text{g C}/\text{cm}^3$ , respectively, and the determination precision of the carbon component was below 5%. Four OC constituents (OC1, OC2, OC3, and OC4) were extracted in a helium atmosphere at temperatures of 140 °C, 280 °C, 480 °C, and 580 °C, respectively. Three EC constituents (EC1, EC2, and EC3) were extracted in a 2% oxygen/98% helium atmosphere at temperatures of 580 °C, 740 °C, and 840 °C, respectively. All of the above analytical processes underwent strict quality control to avoid sample contamination.

#### 2.4. Positive Matrix Factorization Model

The positive matrix factorization (PMF) model is a convenient mathematical approach based on the principle of data error estimation to solve the matrix by the least square method [39]. The contribution of different sources to PM was quantified by analyzing only concentration and uncertainty data files. Because of its effectiveness and accuracy, PMF has been widely applied in the source apportionment of atmospheric pollutants [40]. In this study, Environmental Protection Agency (EPA) PMF version 5.0 was used to explore the potential sectoral sources of PM<sub>1</sub> and PM<sub>2.5</sub> in SJZ. The species input dataset included Na, Mg, Al, Ca, Si, Ti, Cr, Mn, Fe, Ni, Cu, Zn, Sr, Pb, S, Na<sup>+</sup>, NH<sub>4</sub><sup>+</sup>, K<sup>+</sup>, Cl<sup>-</sup>, NO<sub>3</sub><sup>-</sup>, SO<sub>4</sub><sup>2-</sup>, OC, and EC, and some species with abnormal values were excluded to avoid error. The uncertainties of each species were evaluated based on the rules recommended by Paatero et al. [39]. The model was run at least 100 times with different numbers of factors to obtain the optimal solution with minimum Q/Q<sub>exp</sub>. Five sources of PM were finally obtained. The run number is 100 and the Q/Q<sub>exp</sub> is approximately equal to 1.

#### 2.5. Back Trajectory and Clustering Analysis

Hybrid Single Particle Lagrangian Integrated Trajectory (HYSPLIT) version 4.0 was used to backward track the transport pathways of pollutants for SJZ during the study period, and the ARL archives of the National Oceanic and Atmospheric Administration (NOAA) were used as the meteorological input data in this study. The back run time was 48 h with an interval of 1 h, and the tracking height varied from 100 to 6000 m above ground level. A total of 600 trajectories were used for cluster analysis and seven clusters were attained.

#### 2.6. Potential Source Contribution Function Analysis

Potential source contribution function (PSCF) analysis is widely used to identify the regional contributions for receptor sites [41]. In this study, PM<sub>1</sub> and its chemical composition were analyzed, based on the HYSPLIT output trajectories and the MeteoInfo version 1.4.3 model. The study domain was divided into grid cells in the range of 3.86–53.55° N, 73.66–135.04° E, with a horizontal resolution of 0.5° × 0.5°. The 25th and 75th percentile concentrations were considered as the criteria in this study, representing the generally- and heavily-polluted conditions, respectively. The PSCF value in a grid cell was calculated by counting the trajectory segment endpoints that terminate within the cell, and was defined as:

$$PSCF_{ij} = M_{ij} / N_{ij} \cdot W_{ij} \quad (1)$$

where  $N_{ij}$  represents the number of endpoints falling in the  $ij$  cell;  $M_{ij}$  is the number of endpoints in the same cell that corresponds to the pollutant concentration higher than a criterion set by users; and  $W_{ij}$  (Equation (2)) is an empirical weight piecewise function defined by the average number of endpoints  $N_{ave}$ , put forward to reduce the uncertainty produced by small value of  $N_{ij}$ .

$$W_{ij} = \begin{cases} 1.0 & 3N_{ave} \leq N_{ij} \\ 0.7 & 1.5N_{ave} \leq N_{ij} \leq 3N_{ave} \\ 0.4 & N_{ave} \leq N_{ij} \leq 1.5N_{ave} \\ 0.2 & N_{ij} \leq N_{ave} \end{cases} \quad (2)$$

### 3. Results and Discussion

#### 3.1. Chemical Characteristics of PM<sub>1</sub> and PM<sub>2.5</sub>

##### 3.1.1. Mass Concentration of PM

The average mass concentration of PM<sub>1</sub> and PM<sub>2.5</sub> during the study period in SJZ was  $70.51 \pm 47.30 \mu\text{g}/\text{m}^3$  and  $91.68 \pm 54.85 \mu\text{g}/\text{m}^3$ , respectively. The maximum concentrations of PM<sub>1</sub> and PM<sub>2.5</sub> reached  $222.34 \mu\text{g}/\text{m}^3$  and  $261.60 \mu\text{g}/\text{m}^3$ , respectively (Figure 2), approximately 3.0 and 3.5 times the CNAQS for daily PM<sub>2.5</sub> ( $75 \mu\text{g}/\text{m}^3$ ). The ratio of PM<sub>1</sub>/PM<sub>2.5</sub> showed an increasing trend as PM<sub>1</sub> concentration rises (Figure 3a), with a mean value of 0.75, indicating the important role PM<sub>1</sub> played in PM<sub>2.5</sub> pollution, especially for polluted periods. Compared with PM<sub>1</sub> pollution in other studies (Table 1), the average mass concentration in SJZ was dramatically higher than that in other countries—cf.,  $4 \mu\text{g}/\text{m}^3$  in Finland [42] and  $3 \mu\text{g}/\text{m}^3$  in France [43]—and other sites in China—cf.,  $46 \mu\text{g}/\text{m}^3$  in Nanjing [44] and  $41 \mu\text{g}/\text{m}^3$  in Beijing [31]. By summarizing previous studies (Figure 3b) it becomes clear that the percentage of PM<sub>1</sub> in PM<sub>2.5</sub> generally rose as a function of PM<sub>1</sub> concentration, and the ratio in SJZ was higher than in most of the cities (countries). The above evidence indicates that there is severe submicron particulate pollution in SJZ.

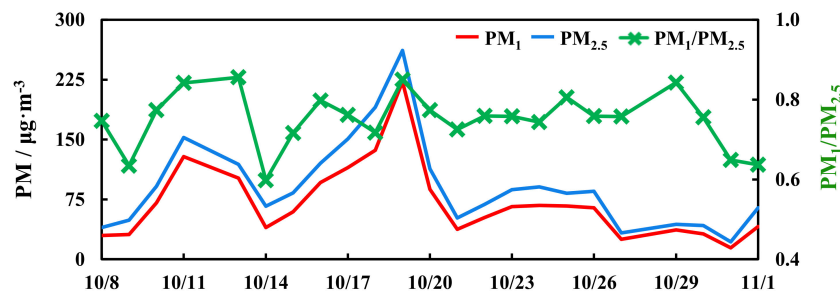


Figure 2. Time series of daily PM concentration and PM<sub>1</sub>/PM<sub>2.5</sub> ratio during the study period.

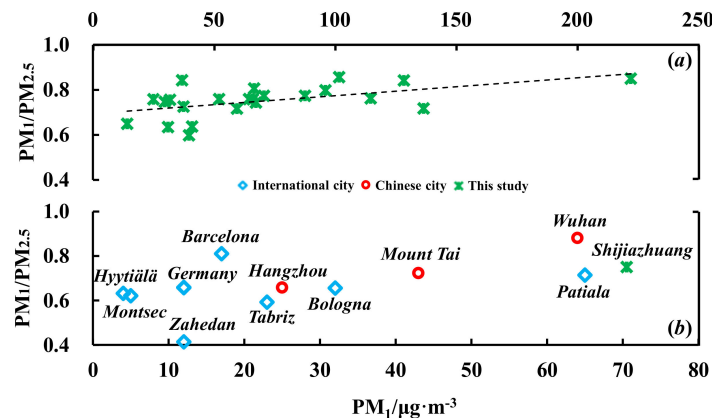


Figure 3. The ratio of PM<sub>1</sub>/PM<sub>2.5</sub> as a function of PM<sub>1</sub> concentration in this study (a) and in other studies (b).

**Table 1.** Average mass concentration of PM<sub>1</sub>, PM<sub>2.5</sub>, and PM<sub>1</sub>/PM<sub>2.5</sub> ratio in autumn.

PM <sub>1</sub> µg·m <sup>-3</sup>	PM <sub>2.5</sub> µg·m <sup>-3</sup>	PM <sub>1</sub> /PM <sub>2.5</sub>	Study Year	City	Country	Reference
62	–	–	2009	Guangzhou	China	[7]
25	38	0.66	2011	Hangzhou	China	[45]
16 <sup>a</sup>	–	–	2011	Hongkong	China	[46]
41	–	–	2012	Beijing	China	[31]
46	–	–	2013	Nanjing	China	[44]
64	73	0.88	2014	Wuhan	China	[47]
43	59	0.72	2014	Mount Tai	China	[48]
<b>71</b>	<b>92</b>	<b>0.75</b>	<b>2016</b>	<b>Shijiazhuang</b>	<b>China</b>	<b>This study</b>
4	6	0.63	2000	Hyytiälä	Finland	[42]
12	19	0.66	2002	Duisburg	Germany	[49]
3	–	–	2006	Puy-de-dôme	France	[43]
17	21	0.81	2007	Barcelona airport	Spain	[50]
12	29	0.41	2008–2009	Zahedan	Iran	[51]
7	–	–	2010	Mediterranean basin	Spain	[52]
32	49	0.66	2011	Bologna	Italy	[53]
23	39	0.59	2012	Tabriz	Iran	[54]
5	8	0.62	2012	Montsec	Spain	[55]
65	91	0.71	2013	Patiala	India	[56]
12	19	0.66	2013	Bologna	Italy	[53]

<sup>a</sup>: PM<sub>1.8</sub>.

### 3.1.2. Characteristics of Chemical Species

The average mass concentration and fractions of 26 species in PM<sub>1</sub> and PM<sub>2.5</sub> from SJZ are listed in Table 2. Water-soluble inorganic ions (WSII) were the dominant component, with concentrations of 28.22 µg/m<sup>3</sup> in PM<sub>1</sub> and 38.52 µg/m<sup>3</sup> in PM<sub>2.5</sub>, respectively. The secondary inorganic aerosols (SIAs) SO<sub>4</sub><sup>2-</sup>, NO<sub>3</sub><sup>-</sup>, and NH<sub>4</sub><sup>+</sup> comprised the largest part of WSII, with concentrations of 9.09 µg/m<sup>3</sup>, 9.08 µg/m<sup>3</sup>, and 7.11 µg/m<sup>3</sup> in PM<sub>1</sub>, respectively, and 11.12 µg/m<sup>3</sup>, 10.55 µg/m<sup>3</sup>, and 7.95 µg/m<sup>3</sup> in PM<sub>2.5</sub>, respectively, implying the significant roles of SIA and secondary sources in fine and submicron particles. Levels of Cl<sup>-</sup>, which is generally identified as the tracer particle of coal burning [57], were non-negligible, with observed concentrations of 1.33 µg/m<sup>3</sup> in PM<sub>1</sub> and 3.69 µg/m<sup>3</sup> in PM<sub>2.5</sub>. For TE, S showed extraordinarily high concentrations of 3.51 µg/m<sup>3</sup> in PM<sub>1</sub> and 3.92 µg/m<sup>3</sup> in PM<sub>2.5</sub>. The concentrations of OC and EC were 12.71 µg/m<sup>3</sup> and 4.99 µg/m<sup>3</sup> in PM<sub>1</sub>, respectively, and 15.43 µg/m<sup>3</sup> and 5.91 µg/m<sup>3</sup> in PM<sub>2.5</sub>, respectively.

Similar profiles were also found in mass fractions as presented in Figure 4, with the order of WSII (40.0%) > OM (28.8%) > EC (7.1%) > TE (6.5%) in PM<sub>1</sub>, and WSII (42.0%) > OM (26.9%) > TE (7.2%) > EC (6.4%) in PM<sub>2.5</sub>, which is consistent with the work of [58]. The concentration of organic matter (OM) was estimated to be 1.6 times that of OC, considering the urban condition and empirical value in SJZ [59]. The lower proportion of TE observed in PM<sub>1</sub> was probably the result of some elements in dust, which were mainly distributed in PM<sub>1-2.5</sub> [60]. The mass fraction ratio of NO<sub>3</sub><sup>-</sup>/SO<sub>4</sub><sup>2-</sup> (~1.0) in SJZ PM<sub>1</sub> was much higher than that in some cities of highly industrialized countries such as Helsinki, Finland (0.04) [61] and Zabrze, Poland (0.16) [11], however, the ratio was lower than in some megacities of China, such as Beijing (1.4) [31] and Nanjing (2.0) [44]. Additionally, a higher proportion of Cl<sup>-</sup> and lower percentage of OM was observed in SJZ than has been reported in some developed countries, such as Sapporo of Japan [62], Atlanta of USA [63] and London of the United Kingdom [64], which illustrates the difference in energy structure among countries with different developmental levels. The fact that a relatively lower percentage of TE (7.2%) and higher percentage of SIA (35.9%) were observed in SJZ than in Kanpur, India (12.8% and 25.9%) shows a clear predominance of secondary pollution in SJZ [65].

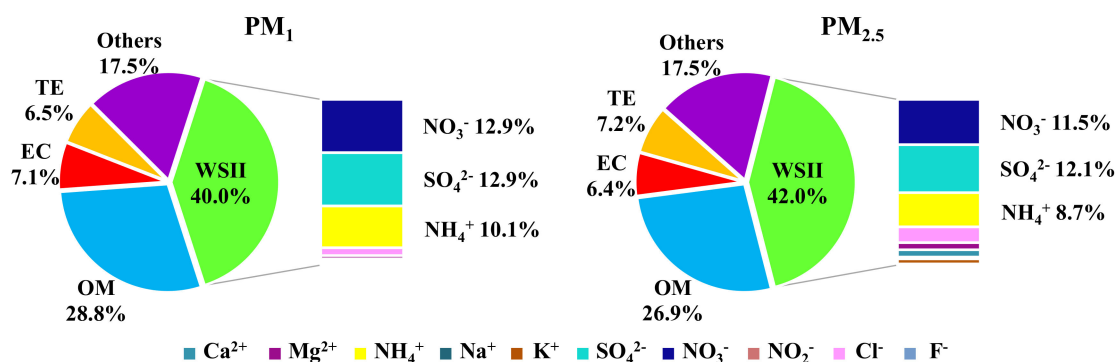


**Figure 4.** The profiles of chemical components in  $PM_{1}$  and  $PM_{2.5}$ . (TE: trace elements; EC: elemental carbon; OM: organic matter; WSII: water-soluble inorganic ions).

**Table 2.** Average mass concentration and standard deviation of chemical species of PM during the study period.

Species	$PM_{1}$		$PM_{2.5}$	
	Average	Standard Deviation	Average	Standard Deviation
PM	70.51	47.30	91.68	54.85
Na	0.30	0.21	0.35	0.23
Mg <sup>b</sup>	28.43	31.26	85.53	65.00
Al	0.04	0.04	0.29	0.28
S	3.51	3.46	3.92	3.60
Ca	0.27	0.32	1.00	1.08
Ti <sup>b</sup>	24.10	12.13	35.91	24.52
Cr <sup>b</sup>	12.99	7.48	19.10	17.12
Mn <sup>b</sup>	19.61	10.38	27.05	16.00
Fe	0.19	0.16	0.53	0.39
Ni <sup>b</sup>	0.30	0.14	0.37	0.18
Cu <sup>b</sup>	13.65	9.10	17.11	10.69
Zn	0.15	0.09	0.18	0.11
Sr <sup>b</sup>	2.35	1.56	3.52	2.35
Pb <sup>b</sup>	65.87	43.04	92.47	71.65
Na <sup>+</sup>	0.24	0.15	0.42	0.33
NH <sub>4</sub> <sup>+</sup>	7.11	6.19	7.95	6.50
K <sup>+</sup>	0.28	0.23	1.18	0.84
Ca <sup>2+</sup>	0.43	0.42	1.71	2.16
Mg <sup>2+</sup>	0.58	0.48	1.63	2.29
F <sup>-</sup>	0.07	0.04	0.19	0.11
Cl <sup>-</sup>	1.33	0.95	3.69	3.49
NO <sub>2</sub> <sup>-</sup>	0.02	0.02	0.06	0.06
NO <sub>3</sub> <sup>-</sup>	9.08	6.65	10.55	6.90
SO <sub>4</sub> <sup>2-</sup>	9.09	6.87	11.12	7.06
OC	12.71	5.23	15.43	5.57
EC	4.99	2.45	5.91	2.62

Units:  $ng/m^3$  for <sup>b</sup>, and  $\mu g/m^3$  for others. (OC: Organic carbon; EC: elemental carbon).

### 3.2. Analysis of $PM_{1}$ in Haze Episodes

According to the air quality standard of  $75 \mu g/m^3$  for daily  $PM_{2.5}$ , we divided the monitoring data into two parts: non-polluted (NP) and polluted (P) levels. As is shown in Table 3, the average mass concentration of  $PM_{1}$  in the polluted period increased to nearly three times the value in the non-polluted period, that is, from  $33.90 \mu g/m^3$  to  $98.67 \mu g/m^3$ , and the same variation was also found in  $PM_{2.5}$ , the concentration of which increased from  $48.06 \mu g/m^3$  in the NP period to  $125.23 \mu g/m^3$  in the P period. The  $PM_{1}/PM_{2.5}$  ratio presented a growth trend from 71.1% in the NP period to 78.1% in the P period, consistent with the previous analysis in Section 3.1.1. The detailed meteorological

conditions for different pollution levels are summarized in Table 3. The meteorological data used in this study were obtained from field observation and from the meteorological data center of the China Meteorological Administration [66]. The lower planetary boundary layer (PBL) height and lower wind speed (WS) were adverse to the diffusion of particles, and much higher relative humidity (RH) may promote the hygroscopic growth of fine particles [67] and then worsen pollution.

A comparison of chemical composition fractions in different pollution levels is presented in Figure 5. It can be seen that the dominant component in the non-polluted period was OM (41.3% in PM<sub>1</sub>, 40.4% in PM<sub>2.5</sub>), and SIA in the polluted period (35.0% in PM<sub>1</sub>, 31.8% in PM<sub>2.5</sub>). Additionally, the variations of SIA contribution from NP to P increased by 0.8% in PM<sub>1</sub>, and decreased by 0.5% in PM<sub>2.5</sub>, indicating the vital function of SIA in the formation of submicron particulate pollution. The decrease of SIA fraction in PM<sub>2.5</sub> may be ascribed to the high proportion of unknown components (named Others in Figure 5), which was likely to be aerosol liquid water related to particle hygroscopicity, and especially to the aqueous-phase reactions of the pollutants in accumulation mode during haze episodes [68]. The percentage of OM in different diameter ranges concurrently decreased even if the mass concentration still increased, consistent with observations from the Yangtze River Delta [38], probably attributed to the extraordinarily percentages of SIA [69]. Alternatively, a weak oxidizing ability of air to organic matter during the haze period may also cause a weak formation of local secondary organic aerosols [70].

**Table 3.** Air quality and meteorological conditions during non-polluted and polluted situations.

Pollutants	Unit	Non-Polluted	Polluted	Average
PM <sub>1</sub>	µg/m <sup>3</sup>	33.90	98.67	70.51
PM <sub>2.5</sub>	µg/m <sup>3</sup>	48.06	125.23	91.68
PM <sub>1</sub> /PM <sub>2.5</sub>	-	0.71	0.78	0.75
Meteorological conditions				
PBL	m	356.1	332.4	342.7
P	hPa	1017.3	1010.8	1013.6
T	°C	10.6	14.9	13.0
RH	%	67.1	79.9	74.3
WS	m/s	1.1	0.9	1.0

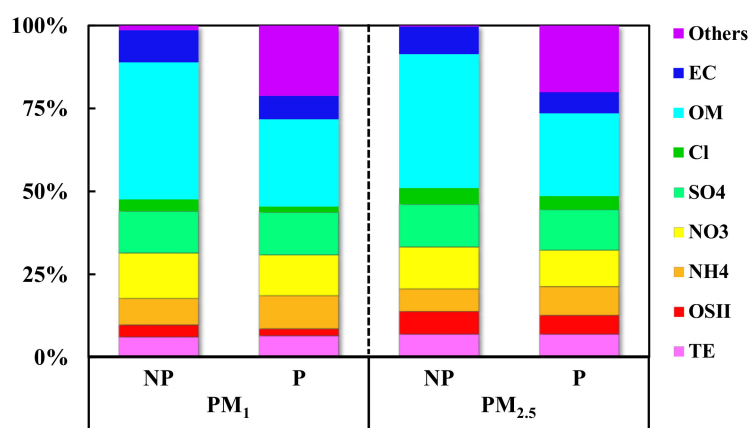


**Figure 5.** The mass fractions of chemical components for different pollution levels (NP: non-polluted; P: polluted; OSII: other soluble inorganic ions; PBL: planetary boundary layer; RH: relative humidity; WS: wind speed).

A further analysis was carried out on the relationship between SIA ions in two typical haze pollution episodes during the study period (Figure 6). The first pollution period (P1) was from 9 to 14 October. Only the mass fraction of NH<sub>4</sub><sup>+</sup> had a relatively synchronous variation with PM<sub>1</sub> concentration (Figure 6a), compared with SO<sub>4</sub><sup>2-</sup> and NO<sub>3</sub><sup>-</sup>. The pollution degree had no

further deterioration, indicating the contribution from accidental sources during P1. The second pollution period (P2) from 15 to 21 October was much more serious than P1, with the maximum concentration of  $PM_{10}$  reaching  $222.34 \mu\text{g}/\text{m}^3$ . As shown in Figure 6a,  $\text{NH}_4^+$  and  $\text{SO}_4^{2-}$  exhibited synchronous variation with  $PM_{10}$  concentration, implying the formation of  $(\text{NH}_4)_2\text{SO}_4$  and/or  $\text{NH}_4\text{HSO}_4$ . The  $[\text{NO}_3^-]/[\text{SO}_4^{2-}]$  ratio of 0.90 suggested that coal combustion may be one of the main sources of heavy haze episodes in SJZ.

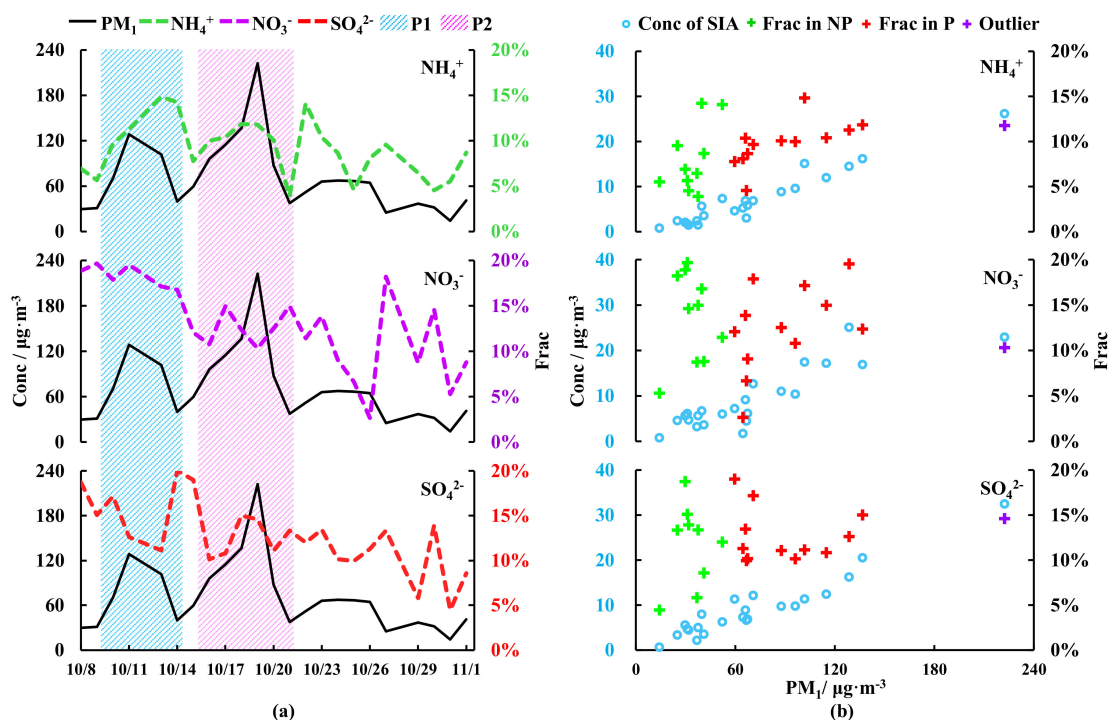


**Figure 6.** Variations in the concentrations and fractions of secondary inorganic aerosol (SIA) (conc: concentration; frac: fraction). (a) The time series of SIA mass fractions related to  $PM_{10}$  concentration; (b) the scatter plot of mass concentration and fractions of SIA as a function of  $PM_{10}$  concentration.

In order to explore the chemical reaction mechanism of SIA during submicron particulate pollution in SJZ, the variations in the daily mass fractions of SIA were displayed as a function of  $PM_{10}$  concentration, as shown in Figure 6b. According to the criterion of  $PM_{2.5}$  for NP and P, the corresponding critical concentration of  $PM_{10}$  in this study was  $60 \mu\text{g}/\text{m}^3$ . For the NP period, the mass fractions of SIA (in green plus sign) varied randomly between 4 and 20%. During the polluted period (in red plus sign), the mean contribution of  $\text{NH}_4^+$  and  $\text{SO}_4^{2-}$  increased by 4%, and  $\text{NO}_3^-$  had a slightly rising trend but with large fluctuation, indicating the vital effect of ammonium and sulfate on  $PM_{10}$  pollution. The tendency observed in this study was generally consistent with that observed in Beijing in autumn [31], opposite to that observed for  $\text{NH}_4^+$ , consistent with that observed for  $\text{SO}_4^{2-}$  and  $\text{NO}_3^-$  in Handan [6] and totally different from that observed in Lanzhou [71]. Nevertheless, an outlier (the purple plus sign) that did not well fit the overall trend appeared at the high concentration range of  $PM_{10}$  ( $>200 \mu\text{g}/\text{m}^3$ ), which may imply another mechanism in the heavier pollution level, although this needs more data and further study.

The above discussion suggests that ammonium played an important role in the formation of haze episodes in SJZ, probably through promoting particle aging and neutralizing acidic substances [70]. Sulfate may be the functional component to worsen the pollution. Different chemical mechanisms for sulfate and nitrate may exist in different degrees of pollution [72]. There are likely to be complicated and region-based chemical mechanisms of the secondary formation of submicron pollution, and further works based on more abundant observations are needed to explore the detailed relationships and interactions between SIA ions.

### 3.3. Sectoral Source Apportionment and Regional Source Identification

Source apportionment is a widely used method to explore the sectoral origins of pollutants. The whole samples of PM<sub>1</sub> and PM<sub>2.5</sub>, from 8 October to 1 November, were analyzed by the PMF model. Between five and seven factors were tested and a five-factor solution was finally chosen (Figure 7a,b).

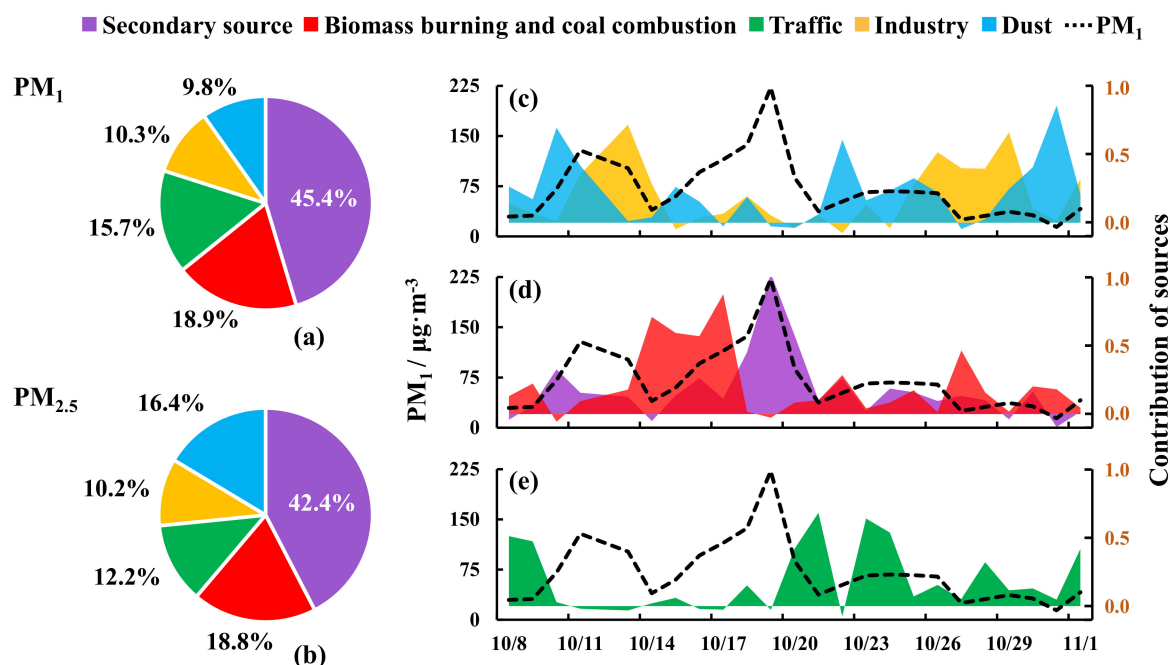


**Figure 7.** Positive matrix factorization (PMF) results of sources and their contributions to PM<sub>1</sub> (a) and PM<sub>2.5</sub> (b), and the time series during the study period (c–e).

Factor 1 was characterized by the high loading of NH<sub>4</sub><sup>+</sup>, NO<sub>3</sub><sup>−</sup>, and SO<sub>4</sub><sup>2−</sup>, and was identified as secondary source (SS), accounting for the largest contribution of 45.4% to PM<sub>1</sub>, 3.0% higher than PM<sub>2.5</sub>, which probably resulted from the size distribution of smaller-diameter secondary components [60]. The time series of contributions from SS (Figure 7d) peaked in the two heavy haze periods, in accordance with the variations of PM<sub>1</sub> concentration, confirming the major contribution of secondary transformation for PM<sub>1</sub> pollution in SJZ.

Factor 2 was classified as the biomass burning and coal combustion source (BB&CC), with about 50% loading of K<sup>+</sup> and Cl<sup>−</sup>, respectively. This factor was the second largest contribution source during the study period, accounting for 18.9% of PM<sub>1</sub> and 18.8% of PM<sub>2.5</sub>. The time series of the contribution from BB&CC peaked at the pollutant accumulation process, especially for P2 (Figure 7d), confirming the contribution of CC concluded in Section 3.2. Coal is the dominant (~70%) energy consumed in SJZ [73], and biomass burning occurred frequently in this harvest season [32]. These made BB&CC sources play a vital role in the occurrence of submicron haze events in SJZ in autumn.

Factor 3 had a distinctly high loading of Cr and Ni, and can be classified as the traffic source (TR), explaining 15.7% of PM<sub>1</sub> and 12.2% of PM<sub>2.5</sub>. Ni is an important component of three-way catalytic converters, and as a result, is widely used as a tracer of traffic sources [74]. Cr was related to driving processes such as road dust and brake wear [75]. The higher proportion of TR in PM<sub>1</sub> may be attributed to ultrafine particles emitted from both diesel- and gasoline-powered engines [76].

Factor 4, with high loading of metallic elements such as Mg, Mn, Fe, Ni, Cu, Zn, and Pb, was classified as the industry source (IN). Mg and Zn are the dominant components of the textile industry in fine particulates [77]; Mn and Fe are associated with steel works [78]; and Ni, Cu, Zn, and Pb are related to industrial processes such as refining, mining, and metal smelting [79,80], which are the dominant industries in the cities of southern Hebei [81]. This source accounted for 10.3% of PM<sub>1</sub>

and 10.2% of PM<sub>2.5</sub>. The time series of peak factor contribution are consistent with P1 (Figure 7c) being the active source for this event.

Factor 5 was recognized as the dust source (DU), and was characterized by Na, Cr, Sr, and Na<sup>+</sup>, which commonly originate from natural sources. Na and Sr were mostly from crustal sources [80], and Na<sup>+</sup> was probably from sea salt [82]. This source accounted for 9.8% of PM<sub>1</sub> and 16.4% of PM<sub>2.5</sub>. The time series of DU contribution also presented a consistent variation of PM<sub>1</sub> concentration during P1 (Figure 7c), indicating the noticeable combined effect of dust and industrial sources for mild or moderate haze pollution in SJZ.

As this is the first study to apportion source contributions to PM<sub>1</sub> in SJZ, an overview of those determined for PM<sub>2.5</sub> is summarized in Table 4 to evaluate the results of this study. The source profile could be explained by about five to six factors, including secondary source, industry, traffic (vehicle), coal combustion, biomass burning, and dust, primarily consistent with this study. As for the autumn source contributions, the results in this study were generally acceptable, compared with the results from Huang et al. [83] and published data from the local government [84]. The higher proportion of secondary source than the annual average level [85] may result from intensive biomass burning during the study period. The lower fraction of traffic may be attributed to stricter vehicle restriction measures during severe air pollution [34]. In contrast with the results of other PM<sub>1</sub> studies, the contribution of secondary source was much higher than that observed in Xi'an [86], but lower for other sources, indicating a greater secondary formation of submicron pollution in SJZ than in cities in Central China. Additionally, the dust source in SJZ also deserves extra attention because of its relatively high percentage in PM<sub>1</sub> compared with Guangzhou [7], which had an equivalent contribution of secondary source.

**Table 4.** Positive matrix factorization (PMF) results of PM<sub>2.5</sub> in Shijiazhuang obtained in previous studies.

Year	Season	SS	IN	TR	CC	BB	DU	Others	Reference
<b>2016</b>	<b>Autumn</b>	<b>42.4</b>	<b>10.2</b>	<b>12.2</b>	<b>18.8</b> <sup>c</sup>		<b>16.4</b>		<b>This study</b>
2013–2014	Annual		17.6–19.4	10.5–11.6	20.0–21.9		15.8–17.3	6.2–6.8	[84]
2013–2014	Annual	15.6	26.8	21.6	11.0		13.4	12.1	[87]
2014	Autumn	52.0	10.0	13.1	5.6	5.6	6.7	6.9	[83]
2014–2015	Annual	36.4	7.0	17.3	15.5	2.8	8.5		[83]
2015–2017	Annual	32.7	5.3	13.4	31.7		19.5	3.3	[85]

<sup>c</sup>: biomass burning and coal combustion. (SS: secondary source; IN: industry source; TR: traffic/vehicle source; CC: coal combustion; BB: biomass burning; DU: dust).

The regional contributions to PM<sub>1</sub> are presented in Figure 8. For the general condition (Figure 8a), local southern Hebei, mid-eastern Shanxi, and northern Henan were the major contribution regions for SJZ PM<sub>1</sub> during the study period. The local SJZ and neighbor cities in Shanxi distinctly accounted for the main regional contribution during the polluted period (Figure 8b), which suggests that combined control plans in PM pollution should be carried out to effectively mitigate the severity of haze episodes in this area. To understand the regional distribution of the two biggest sectoral sources for SJZ (SS and BB&CC), PSCF analysis was also performed for SIA, K<sup>+</sup>, and Cl<sup>-</sup> (Figure 8c–g). For NH<sub>4</sub><sup>+</sup> and NO<sub>3</sub><sup>-</sup>, neighboring cities in northern Henan may be responsible for the dominant contribution, while for SO<sub>4</sub><sup>2-</sup> some regions in Shanxi and Shandong should also be considered, probably because of the high levels of heavy industry in these areas [88]. The regions along the border of Henan and Shandong were the major contributors of K<sup>+</sup> and Cl<sup>-</sup> during the study period and fit well with the distribution of biomass burning activities [32] and coal consumptions [73]. Furthermore, the contribution from the regions around Beijing, Langfang, and Tianjin to coal combustion should also be taken into account according to the results of the Cl<sup>-</sup> analysis.

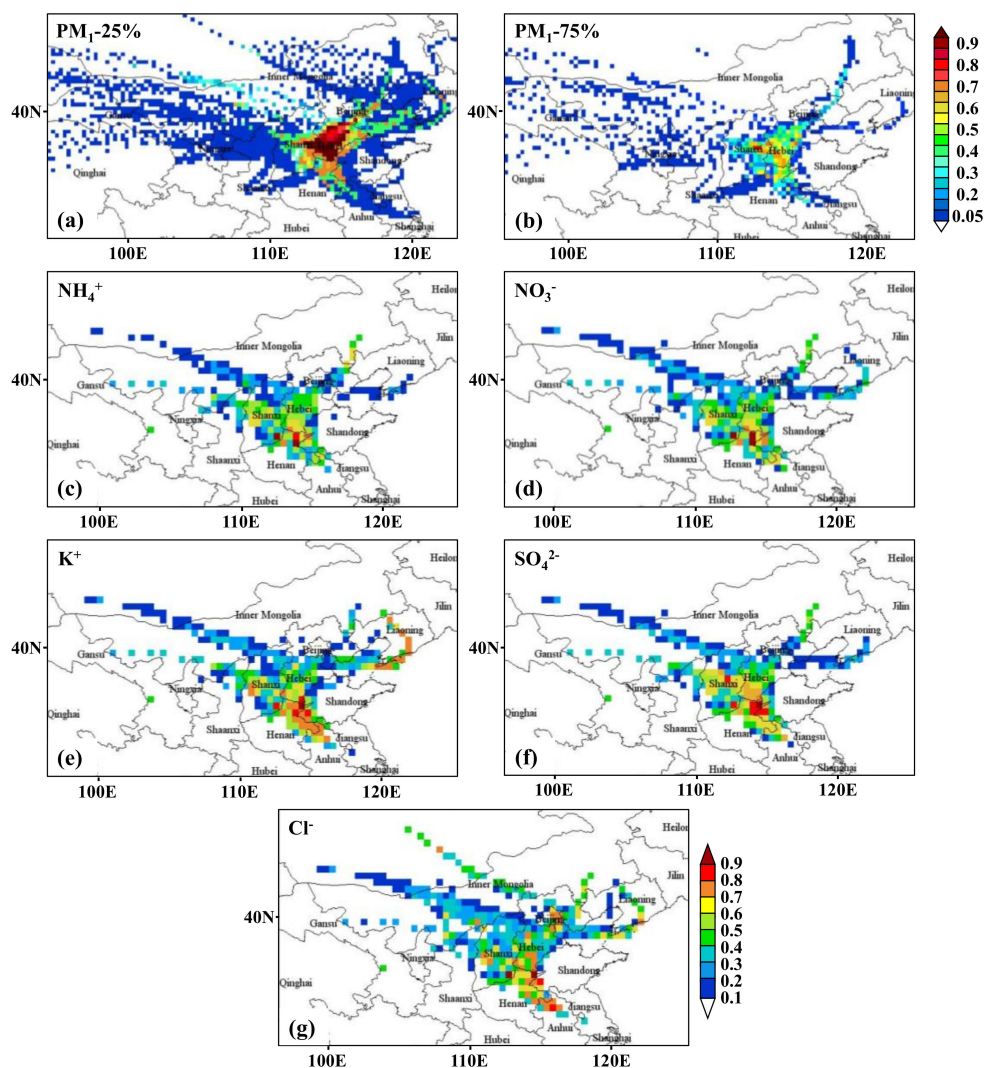


**Figure 8.** Potential source contribution function (PSCF) analysis results for regional contributions to SJZ under the criterion of 25th percentage  $PM_{10}$  concentration (a), and 75th percentage  $PM_{10}$  concentration (b),  $NH_4^+$  concentration (c),  $NO_3^-$  concentration (d),  $SO_4^{2-}$  concentration (e),  $K^+$  concentration (f), and  $Cl^-$  concentration (g).

### 3.4. Chemical Distribution and Transport Pathways

To clarify the chemical characteristics of different contribution regions, 600  $PM_{10}$  trajectories were analyzed using the HYSPLIT model, and seven clusters were finally obtained (Figure 9). The corresponding  $PM_{10}$  concentration of each cluster was ranked in the order of Cluster 4 (C4,  $93.96 \mu g/m^3$ ) > Cluster 5 (C5,  $83.59 \mu g/m^3$ ) > Cluster 7 (C7,  $82.58 \mu g/m^3$ ) > Cluster 1 (C1,  $63.43 \mu g/m^3$ ) > Cluster 6 (C6,  $63.19 \mu g/m^3$ ) > Cluster 3 (C3,  $36.47 \mu g/m^3$ ) > Cluster 2 (C2,  $31.28 \mu g/m^3$ ). C4 and C6 were the dominant clusters during the study period, with the sum of number contribution accounting for nearly 60% of the total, followed by C2 and C3; other clusters shared only a small part.

C1 and C2 represented the areas located in the northwest of SJZ, including middle Hebei and most parts of Inner Mongolia province. Although the average  $PM_{10}$  concentration was classified at a polluted level ( $>60 \mu g/m^3$ ), the long-range transport weakened the contribution of C1 and C2 (19%), which may not be the major contribution pathways for SJZ during the study period.

C3 and C6 mainly represented the northern and northeastern contribution regions for SJZ. C3 was apparently a continuation of C6, transporting through central Inner Mongolia from north to southeast, and then traversing the BTH region from east to southwest. The curving path is likely attributable to

the special terrain and location of this area as shown in Figure 1b. The proportion of OC in PM<sub>1</sub> under these two pathways was relatively high. C6 mainly represented the mid-BTH region, involving several heavily polluted cities such as Tangshan (TS), Tianjin (TJ), Langfang (LF), and Baoding (BD). Previous studies showed the component of OC in this area was mostly emitted from fuel (e.g., coal and oil) burning [83]. Among the cities, TJ had a substantial vehicle population of 2.74 million in 2016 [89] and TS is famous for its steel production, powered by great quantities of coal burning [90]. These suggested vital contributions of fossil fuel burning sources from mid-BHT to SJZ during the study period.

C4 and C5 were the airflows from the northwest of SJZ. Similar to the relationship of C3 and C6, C5 was also a continuation of C4, from as far as Gansu and Ningxia provinces, meeting with C4 in Shanxi, and after crossing northern Hebei, finally arrived in SJZ. It was a typical pathway across the Taihang Mountains, with a transport height of over 3000 m above ground level. The concentration of SIA, OC, and EC in these two pathways were much higher than those in northern clusters, indicating a greater contribution from southern cities to SJZ. C4 mainly represented southern Hebei including local SJZ and eastern Shanxi, accounting for a higher proportion and mass concentration of PM<sub>1</sub> than all other clusters. C4 was occupied with extremely high mass concentrations of SIA and OC, implying that secondary source from local southern Hebei and regional transport from eastern Shanxi [91] played significant roles in haze events in SJZ.

C7 was another curving pathway from the southeast of SJZ. It was probably shaped by the special terrain (plain is surrounded by mountains in west and south) of NCP, including Henan, Shandong, Anhui, and Jiangsu province (Figure 1b). As well as for SIA and OC, C7 also had a relatively higher concentration of K<sup>+</sup> (0.53 µg/m<sup>3</sup>) compared with other clusters, and as K<sup>+</sup> is widely used as the tracer of biomass burning source, this result indicates a considerable contribution of biomass burning from southern NCP to SJZ. This observation was consistent with the conclusion made in Section 3.3. Heavy agricultural activities in the passing regions of C7 could explain the high concentration of PM<sub>1</sub> of C7.

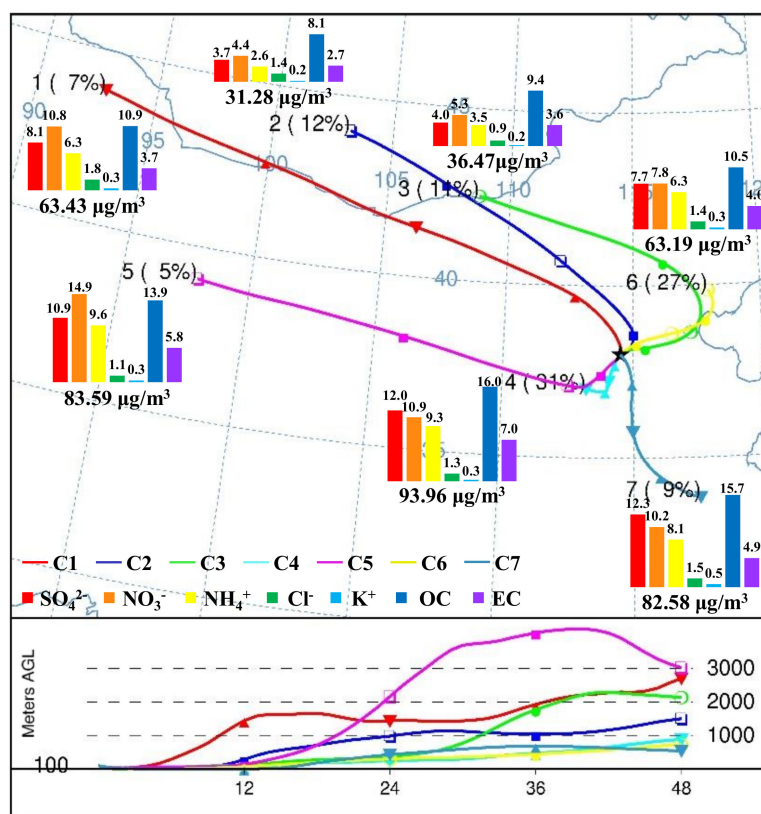


**Figure 9.** Seven 48-h air particle backward trajectory clusters and the corresponding PM<sub>1</sub> characteristics (AGL: above ground level).

In order to identify the contributions of each cluster to haze episodes in SJZ, two heavy polluted events (peak  $PM_{2.5}$  concentration  $>150 \mu\text{g}/\text{m}^3$ ), which happened during the study period, were chosen to analyze the detailed processes (Figure 10). Because of the lack of hourly  $PM_1$  data, hourly  $PM_{2.5}$  concentrations were collected from the published data of the Ministry of Environmental Protection [92] for the further analysis. P1 occurred between 16:00 on 10 October and 20:00 on 13 October, with a duration of 77 h and a peak  $PM_{2.5}$  concentration of  $253 \mu\text{g}/\text{m}^3$  (Figure 10a). P2 occurred between 18:00 on 15 October and 14:00 on 20 October, with a duration of 117 h and a peak  $PM_{2.5}$  concentration of  $321 \mu\text{g}/\text{m}^3$  (Figure 10b). It can clearly be seen that during the pollutant accumulation period (in red shadow), C4 and C6 were the major contribution clusters both for P1 and P2, confirming the analysis discussed above. Additionally, C5 and C7 were probably other potential transport paths for pollutants for P1 and P2, respectively, because these two pathways raised the concentration of  $PM_{2.5}$  from NP to P condition at the beginning. For the clear process of pollutants (in green shadow), there was a difference between P1 and P2. The relatively clean airflow from C5 decreased the  $PM_{2.5}$  concentration of P1. In P2, the airflow from C7 may reduce the severity of the heavy haze.

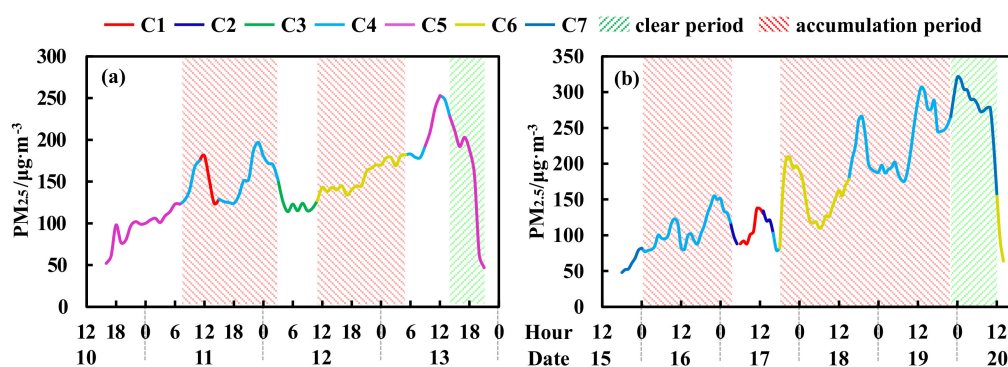


**Figure 10.** The dominant contributions of seven transport pathways during the haze episodes of (a) period 1 and (b) period 2.

#### 4. Conclusions

Submicron particulate ( $PM_1$ ) pollution became an increasingly serious issue with the development of research on heavy haze episodes in China. However, there have been few studies on the characteristics of  $PM_1$  pollution in Shijiazhuang (SJZ), which is one of the most polluted cities in China and in the world. Therefore, an intensive campaign to simultaneously sample  $PM_1$  and  $PM_{2.5}$  was conducted during autumn 2016 in SJZ.

The results show that SJZ suffers from severe submicron pollution. The average mass concentrations of  $PM_1$  and  $PM_{2.5}$  were found to be  $70.51 \pm 47.30 \mu\text{g}/\text{m}^3$  and  $91.68 \pm 54.85 \mu\text{g}/\text{m}^3$ , respectively, higher than most sites in the world. The average ratio of  $PM_1/PM_{2.5}$  was 0.75 during the study period in SJZ, which ranked highly compared with previous studies, and had an increasing trend as a function of  $PM_1$  concentration. WSII (especially SIA) were the dominant component in both  $PM_1$  (40.0%) and  $PM_{2.5}$  (42.0%), followed by OM (28.8% in  $PM_1$ , 26.9% in  $PM_{2.5}$ ) and EC (7.1% in  $PM_1$ , 6.4% in  $PM_{2.5}$ ). The mass fractions of TE (6.5% in  $PM_1$ , 7.2% in  $PM_{2.5}$ ) were lower than those of EC in  $PM_1$ , but higher in  $PM_{2.5}$ .

SIA is found to be the key component for the formation of  $PM_1$  pollution in SJZ. The profiles of chemical compositions in non-polluted and polluted periods had similar variations in both  $PM_1$  and  $PM_{2.5}$  with the exception of SIA, which increased by 0.8% in  $PM_1$  and decreased by 0.5% in  $PM_{2.5}$ , suggesting the importance of SIA in the formation of submicron particulate pollution. Further analysis of SIA in  $PM_1$  found that  $\text{NH}_4^+$  promoted the occurrence of haze pollution in SJZ, while  $\text{SO}_4^{2-}$  and  $\text{NO}_3^-$  worsened the pollution by different chemical mechanisms as the  $PM_1$  concentration rose. Different pollution levels may also be driven by different chemical mechanisms.

The first ever source apportionment of PM<sub>1</sub> in SJZ was carried out in this study. The sectoral sources analysis showed that the major sources of haze pollution for SJZ were the following: (1) secondary source, (2) biomass burning and coal combustion, (3) traffic, (4) industry, and (5) dust, with percentages of 45.4%, 18.9%, 15.7%, 10.3%, and 9.8%, respectively, being observed in PM<sub>1</sub>, and 42.4%, 18.8%, 12.2%, 10.2%, and 16.4%, respectively, being observed in PM<sub>2.5</sub>. Regional source identification showed that local southern Hebei, mid-eastern Shanxi, and northern Henan were the dominant functional areas during the study period. Moreover, cluster analysis showed that three transport pathways, including the airflow from Shanxi with the secondary source (C4), the airflow from mid-BTH region with the fuel burning source (C6), and the airflow from southern NCP with the biomass burning source (C7), should be given more attention during combined control to weaken the severity of haze pollution in SJZ.

This study carried out a detailed and systematic analysis of submicron pollution in a heavily polluted city, which explored the chemical characteristics of PM<sub>1</sub> and PM<sub>2.5</sub>, emphasized the importance of SIA on the mitigation of PM<sub>1</sub> pollution, and identified the source and regional contributions for haze pollution. However, because of the limitation of the dataset, there are inevitably some uncertainties in this analysis, such as source apportionment and trajectory clustering, and, therefore, more samples would be better for more refined and precise research on PM<sub>1</sub> pollution.

**Author Contributions:** Methodology, Ya.Z.; Validation, Yi.Z. and D.C.; Formal Analysis, S.L.; Resources, H.W.; Data Curation, H.Z.; Writing—Original Draft Preparation, S.L.; Writing—Review & Editing, J.L.; Visualization, S.L.; Supervision, S.C.

**Funding:** This research was supported by the Natural Sciences Foundation of China (No. 91644110 & 51878012), the Key Projects on Heavy Air Pollution Control (DQGG0303), and the New Talent Program of Beijing University of Technology (No. 2017-RX(1)-10).

**Acknowledgments:** We greatly appreciated Beijing Municipal Commission of Education and Beijing Municipal Commission of Science and Technology for supporting this work. The authors are grateful to the anonymous reviewers for their insightful comments.

**Conflicts of Interest:** The authors declare no conflict of interest.

## References

1. Han, R.; Wang, S.; Shen, W.; Wang, J.; Wu, K.; Ren, Z.; Feng, M. Spatial and temporal variation of haze in China from 1961 to 2012. *J. Environ. Sci.* **2016**, *46*, 134–146. [[CrossRef](#)] [[PubMed](#)]
2. Qiao, X.; Ying, Q.; Li, X.H.; Zhang, H.L.; Hu, J.L.; Tang, Y.; Chen, X. Source apportionment of PM<sub>2.5</sub> for 25 Chinese provincial capitals and municipalities using a source-oriented Community Multiscale Air Quality model. *Sci. Total Environ.* **2018**, *612*, 462–471. [[CrossRef](#)] [[PubMed](#)]
3. Singh, A.; Bloss, W.J.; Pope, F.D. 60 years of UK visibility measurements: Impact of meteorology and atmospheric pollutants on visibility. *Atmos. Chem. Phys.* **2017**, *17*, 2085–2101. [[CrossRef](#)]
4. Zhang, J.; Liu, Y.; Cui, L.L.; Liu, S.Q.; Yin, X.X.; Li, H.C. Ambient air pollution, smog episodes and mortality in Jinan, China. *Sci. Rep.* **2017**, *7*. [[CrossRef](#)] [[PubMed](#)]
5. Yao, L. Causative impact of air pollution on evapotranspiration in the North China Plain. *Environ. Res.* **2017**, *158*, 436–442. [[CrossRef](#)] [[PubMed](#)]
6. Li, H.; Zhang, Q.; Zhang, Q.; Chen, C.; Wang, L.; Wei, Z.; Zhou, S.; Parworth, C.; Zheng, B.; Canonaco, F.; et al. Wintertime aerosol chemistry and haze evolution in an extremely polluted city of the North China Plain: Significant contribution from coal and biomass combustion. *Atmos. Chem. Phys.* **2017**, *17*, 4751–4768. [[CrossRef](#)]
7. Tao, J.; Shen, Z.X.; Zhu, C.S.; Yue, J.H.; Cao, J.J.; Liu, S.X.; Zhu, L.H.; Zhang, R.J. Seasonal variations and chemical characteristics of sub-micrometer particles (PM<sub>1</sub>) in Guangzhou, China. *Atmos. Res.* **2012**, *118*, 222–231. [[CrossRef](#)]
8. Wang, Y.C.; Huang, R.J.; Ni, H.Y.; Chen, Y.; Wang, Q.Y.; Li, G.H.; Tie, X.X.; Shen, Z.X.; Huang, Y.; Liu, S.X.; et al. Chemical composition, sources and secondary processes of aerosols in Baoji city of northwest China. *Atmos. Environ.* **2017**, *158*, 128–137. [[CrossRef](#)]

9. Zhang, J.K.; Cheng, M.T.; Ji, D.S.; Liu, Z.R.; Hu, B.; Sun, Y.; Wang, Y.S. Characterization of submicron particles during biomass burning and coal combustion periods in Beijing, China. *Sci. Total Environ.* **2016**, *562*, 812–821. [[CrossRef](#)] [[PubMed](#)]
10. Filep, A.; Fodor, G.H.; Kun-Szabo, F.; Tiszlavicz, L.; Razga, Z.; Bozso, G.; Bozoki, Z.; Szabo, G.; Petak, F. Exposure to urban PM<sub>1</sub> in rats: Development of bronchial inflammation and airway hyperresponsiveness. *Respir. Res.* **2016**, *17*. [[CrossRef](#)] [[PubMed](#)]
11. Widziewicz, K.; Rogula-Kozłowska, W.; Rogula-Kopiec, P.; Majewski, G.; Loska, K. PM<sub>1</sub> and PM<sub>1</sub>-bound metals during dry and wet periods: Ambient concentration and health effects. *Environ. Eng. Sci.* **2017**, *34*. [[CrossRef](#)]
12. van Drooge, B.L.; Marqueno, A.; Grimalt, J.O.; Fernandez, P.; Porte, C. Comparative toxicity and endocrine disruption potential of urban and rural atmospheric organic PM<sub>1</sub> in JEG-3 human placental cells. *Environ. Pollut.* **2017**, *230*, 378–386. [[CrossRef](#)] [[PubMed](#)]
13. Singh, D.K.; Gupta, T. Source apportionment and risk assessment of PM, bound trace metals collected during foggy and non-foggy episodes at a representative site in the Indo-Gangetic plain. *Sci. Total Environ.* **2016**, *550*, 80–94. [[CrossRef](#)] [[PubMed](#)]
14. Chang, L.T.; Tang, C.S.; Pan, Y.Z.; Chan, C.C. Association of heart rate variability of the elderly with personal exposure to PM<sub>1</sub>, PM<sub>1-2.5</sub>, and PM<sub>2.5-10</sub>. *B. Environ. Contam. Tox.* **2007**, *79*, 552–556. [[CrossRef](#)] [[PubMed](#)]
15. Talbi, A.; Kerchich, Y.; Kerbachi, R.; Boughedaoui, M. Assessment of annual air pollution levels with PM<sub>1</sub>, PM<sub>2.5</sub>, PM<sub>10</sub> and associated heavy metals in Algiers, Algeria. *Environ. Pollut.* **2018**, *232*, 252–263. [[CrossRef](#)] [[PubMed](#)]
16. Yausheva, E.P.; Kozlov, V.S.; Belan, B.D.; Arshinov, M.Y.; Chernov, D.G.; Shmargunov, V.P. In differences in seasonal average concentrations of aerosol and black carbon and particle size distributions from the data of monitoring in tomsk and under background conditions in 2014–2015. In Proceedings of the 22nd International Symposium on Atmospheric and Ocean Optics—Atmospheric Physics, Tomsk, Russia, 30 June–3 July 2016.
17. Sun, Y.; Xu, W.; Zhang, Q.; Jiang, Q.; Canonaco, F.; Prevot, A.S.H.; Fu, P.; Li, J.; Jayne, J.; Worsnop, D.R.; et al. Source apportionment of organic aerosol from 2-year highly time-resolved measurements by an aerosol chemical speciation monitor in Beijing, China. *Atmos. Chem. Phys.* **2018**, *18*, 8469–8489. [[CrossRef](#)]
18. Ji, D.; Zhang, J.; He, J.; Wang, X.; Pang, B.; Liu, Z.; Wang, L.; Wang, Y. Characteristics of atmospheric organic and elemental carbon aerosols in urban Beijing, China. *Atmos. Environ.* **2016**, *125*, 293–306. [[CrossRef](#)]
19. Wang, L.; Wen, T.X.; Miao, H.Y.; Gao, W.K.; Wang, Y.S. Concentrations and size distributions of water-soluble inorganic ions in aerosol particles in Taiyuan, Shanxi. *Environ. Sci.* **2016**, *9*, 3249–3257.
20. Pan, Y.; Wang, Y.; Zhang, J.; Liu, Z.; Wang, L.; Tian, S.; Tang, G.; Gao, W.; Ji, D.; Song, T.; et al. Redefining the importance of nitrate during haze pollution to help optimize an emission control strategy. *Atmos. Environ.* **2016**, *141*, 197–202. [[CrossRef](#)]
21. Sun, Y.; Jiang, Q.; Xu, Y.; Ma, Y.; Zhang, Y.; Liu, X.; Li, W.; Wang, F.; Li, J.; Wang, P.; et al. Aerosol characterization over the North China Plain: Haze life cycle and biomass burning impacts in summer. *J. Geophys. Res. Atmos.* **2016**, *121*, 2508–2521. [[CrossRef](#)]
22. Lee, B.P.; Wang, H.; Chan, C.K. Diurnal and day-to-day characteristics of ambient particle mass size distributions from HR-ToF-AMS measurements at an urban site and a suburban site in Hong Kong. *Atmos. Chem. Phys.* **2017**, *17*, 13605–13624. [[CrossRef](#)]
23. Du, W.; Zhao, J.; Wang, Y.; Zhang, Y.; Wang, Q.; Xu, W.; Chen, C.; Han, T.; Zhang, F.; Li, Z.; et al. Simultaneous measurements of particle number size distributions at ground level and 260 m on a meteorological tower in urban Beijing, China. *Atmos. Chem. Phys.* **2017**, *17*, 6797–6811. [[CrossRef](#)]
24. Arndt, J.; Sciare, J.; Mallet, M.; Roberts, G.C.; Marchand, N.; Sartelet, K.; Sellegri, K.; Dulac, F.; Healy, R.M.; Wenger, J.C. Sources and mixing state of summertime background aerosol in the north-western Mediterranean basin. *Atmos. Chem. Phys.* **2017**, *17*, 6975–7001. [[CrossRef](#)]
25. Caggiano, R.; Macchiato, M.; Trippetta, S. Levels, chemical composition and sources of fine aerosol particles (PM<sub>1</sub>) in an area of the Mediterranean basin. *Sci. Total Environ.* **2010**, *408*, 884–895. [[CrossRef](#)] [[PubMed](#)]
26. Zhang, Y.; Lang, J.; Cheng, S.; Li, S.; Zhou, Y.; Chen, D.; Zhang, H.; Wang, H. Chemical composition and sources of PM<sub>1</sub> and PM<sub>2.5</sub> in Beijing in autumn. *Sci Total Environ.* **2018**, *630*, 72–82. [[CrossRef](#)] [[PubMed](#)]
27. The Official Website of China National Environmental Monitoring Centre. Available online: <http://www.cnemc.cn/> (accessed on 6 August 2018).

28. The Official Website of Shijiazhuang Environmental Protection Bureau. Available online: <http://www.sjzhb.gov.cn/> (accessed on 6 August 2018).
29. Wang, Y.; Bao, S.; Wang, S.; Hu, Y.; Shi, X.; Wang, J.; Zhao, B.; Jiang, J.; Zheng, M.; Wu, M.; et al. Local and regional contributions to fine particulate matter in Beijing during heavy haze episodes. *Sci. Total Environ.* **2017**, *580*, 283–296. [[CrossRef](#)] [[PubMed](#)]
30. Maji, K.J.; Arora, M.; Dikshit, A.K. Burden of disease attributed to ambient PM<sub>2.5</sub> and PM<sub>10</sub> exposure in 190 cities in China. *Environ. Sci. Pollut. Res.* **2017**, *24*, 11559–11572. [[CrossRef](#)] [[PubMed](#)]
31. Hu, W.; Hu, M.; Hu, W.W.; Zheng, J.; Chen, C.; Wu, Y.S.; Guo, S. Seasonal variations in high time-resolved chemical compositions, sources, and evolution of atmospheric submicron aerosols in the megacity Beijing. *Atmos. Chem. Phys.* **2017**, *17*, 9979–10000. [[CrossRef](#)]
32. Zhou, Y.; Xing, X.; Lang, J.; Chen, D.; Cheng, S.; Wei, L.; Wei, X.; Liu, C. A comprehensive biomass burning emission inventory with high spatial and temporal resolution in China. *Atmos. Chem. Phys.* **2017**, *17*, 2839–2864. [[CrossRef](#)]
33. Chen, J.; Li, C.; Ristovski, Z.; Milic, A.; Gu, Y.; Islam, M.S.; Wang, S.; Hao, J.; Zhang, H.; He, C.; et al. A review of biomass burning: Emissions and impacts on air quality, health and climate in China. *Sci. Total Environ.* **2017**, *579*, 1000–1034. [[CrossRef](#)] [[PubMed](#)]
34. The Official Website of Shijiazhuang Municipal People’s Government. Available online: <http://www.sjz.gov.cn/> (accessed on 6 August 2018).
35. Shijiazhuang Municipal Bureau of Statistics. *Shijiazhuang Statistical Yearbook*; China Statistics Press: Beijing, China, 2016.
36. Shijiazhuang Municipal People’s Government. Heat Supply Regulations in Shijiazhuang. Available online: <http://www.sjz.gov.cn/col/1497948667745/2013/06/05/1497954766982.html> (accessed on 4 September 2018).
37. Zhao, X.J.; Zhao, P.S.; Xu, J.; Meng, W.; Pu, W.W.; Dong, F.; He, D.; Shi, Q.F. Analysis of a winter regional haze event and its formation mechanism in the North China Plain. *Atmos. Chem. Phys.* **2013**, *13*, 5685–5696. [[CrossRef](#)]
38. Tang, L.; Yu, H.; Ding, A.; Zhang, Y.; Qin, W.; Wang, Z.; Chen, W.; Hua, Y.; Yang, X. Regional contribution to PM<sub>1</sub> pollution during winter haze in Yangtze River Delta, China. *Sci. Total Environ.* **2016**, *541*, 161–166. [[CrossRef](#)] [[PubMed](#)]
39. Paatero, P. Least squares formulation of robust non-negative factor analysis. *Chem. Intell. Lab. Syst.* **1997**, *37*, 23–35. [[CrossRef](#)]
40. Tao, J.; Zhang, L.; Cao, J.; Zhang, R. A review of current knowledge concerning PM<sub>2.5</sub> chemical composition, aerosol optical properties and their relationships across China. *Atmos. Chem. Phys.* **2017**, *17*, 9485–9518. [[CrossRef](#)]
41. Argyropoulos, G.; Samara, C.; Diapouli, E.; Eleftheriadis, K.; Papaoikonomou, K.; Kungolos, A. Source apportionment of PM<sub>10</sub> and PM<sub>2.5</sub> in major urban Greek agglomerations using a hybrid source-receptor modeling process. *Sci. Total Environ.* **2017**, *601*, 906–917. [[CrossRef](#)] [[PubMed](#)]
42. Laakso, L.; Hussein, T.; Aarnio, P.; Komppula, M.; Hiltunen, V.; Viisanen, Y.; Kulmala, M. Diurnal and annual characteristics of particle mass and number concentrations in urban, rural and Arctic environments in Finland. *Atmos. Environ.* **2003**, *37*, 2629–2641. [[CrossRef](#)]
43. Bourcier, L.; Sellegri, K.; Chausse, P.; Pichon, J.M.; Laj, P. Seasonal variation of water-soluble inorganic components in aerosol size-segregated at the puy de Dome station (1,465 m a.s.l.), France. *J. Atmos. Chem.* **2012**, *69*, 47–66. [[CrossRef](#)]
44. Zhang, Y.J.; Tang, L.L.; Wang, Z.; Yu, H.X.; Sun, Y.L.; Liu, D.; Qin, W.; Canonaco, F.; Prevot, A.S.H.; Zhang, H.L.; et al. Insights into characteristics, sources, and evolution of submicron aerosols during harvest seasons in the Yangtze River delta region, China. *Atmos. Chem. Phys.* **2015**, *15*, 1331–1349. [[CrossRef](#)]
45. Li, X.; Zhang, R.; Cong, X.; Cheng, L.; Liu, J.; Xu, H. Characterization of the size-segregated inorganic compounds in Lin’an, a regional atmosphere background station in the Yangtze River Delta region. *Atmos. Pollut. Res.* **2015**, *6*, 1058–1065. [[CrossRef](#)]
46. Li, Y.J.; Lee, B.P.; Su, L.; Fung, J.C.H.; Chan, C.K. Seasonal characteristics of fine particulate matter (PM) based on high-resolution time-of-flight aerosol mass spectrometric (HR-ToF-AMS) measurements at the HKUST Supersite in Hong Kong. *Atmos. Chem. Phys.* **2015**, *15*, 37–53. [[CrossRef](#)]

47. Gong, W.; Zhang, T.H.; Zhu, Z.M.; Ma, Y.Y.; Ma, X.; Wang, W. Characteristics of PM<sub>1.0</sub>, PM<sub>2.5</sub>, and PM<sub>10</sub>, and Their Relation to Black Carbon in Wuhan, Central China. *Atmosphere* **2015**, *6*, 1377–1387. [[CrossRef](#)]
48. Zhao, T.; Yang, L.X.; Yan, W.D.; Zhang, J.M.; Lu, W.; Yang, Y.M.; Chen, J.M.; Wang, W.X. Chemical characteristics of PM<sub>1</sub>/PM<sub>2.5</sub> and influence on visual range at the summit of Mount Tai, North China. *Sci. Total Environ.* **2017**, *575*, 458–466. [[CrossRef](#)] [[PubMed](#)]
49. Pennanen, A.S.; Sillanpaa, M.; Hillamo, R.; Quass, U.; John, A.C.; Branis, M.; Hunova, I.; Meliefste, K.; Janssen, N.A.H.; Koskentalo, T.; et al. Performance of a high-volume cascade impactor in six European urban environments: Mass measurement and chemical characterization of size-segregated particulate samples. *Sci. Total Environ.* **2007**, *374*, 297–310. [[CrossRef](#)] [[PubMed](#)]
50. Amato, F.; Moreno, T.; Pandolfi, M.; Querol, X.; Alastuey, A.; Delgado, A.; Pedrero, M.; Cots, N. Concentrations, sources and geochemistry of airborne particulate matter at a major European airport. *J. Environ. Monit.* **2010**, *12*, 854–862. [[CrossRef](#)] [[PubMed](#)]
51. Rashki, A.; Rautenbach, C.J.D.; Eriksson, P.G.; Kaskaoutis, D.G.; Gupta, P. Temporal changes of particulate concentration in the ambient air over the city of Zahedan, Iran. *Air Qual. Atmos. Health.* **2013**, *6*, 123–135. [[CrossRef](#)]
52. Nicolas, J.F.; Galindo, N.; Yubero, E.; Crespo, J.; Soler, R. PM<sub>1</sub> variability and transport conditions between an urban coastal area and a high mountain site during the cold season. *Atmos. Environ.* **2015**, *118*, 127–134. [[CrossRef](#)]
53. Bocchi, C.; Bazzini, C.; Fontana, F.; Pinto, G.; Martino, A.; Cassoni, F. Characterization of urban aerosol: Seasonal variation of mutagenicity and genotoxicity of PM<sub>2.5</sub>, PM<sub>1</sub> and semi-volatile organic compounds. *Mutation Res. Genet. Toxicol. Environ. Mutagen.* **2016**, *809*, 16–23. [[CrossRef](#)] [[PubMed](#)]
54. Gholampour, A.; Nabizadeh, R.; Naseri, S.; Yunesian, M.; Taghipour, H.; Rastkari, N.; Nazmara, S.; Faridi, S.; Mahvi, A.H. Exposure and health impacts of outdoor particulate matter in two urban and industrialized area of Tabriz, Iran. *J. Environ. Sci. Health. Eng.* **2014**, *12*, 27. [[CrossRef](#)] [[PubMed](#)]
55. Ripoll, A.; Pey, J.; Minguillon, M.C.; Perez, N.; Pandolfi, M.; Querol, X.; Alastuey, A. Three years of aerosol mass, black carbon and particle number concentrations at Montsec (southern Pyrenees, 1570 m a.s.l.). *Atmos. Chem. Phys.* **2014**, *14*, 4279–4295. [[CrossRef](#)]
56. Singh, A.; Rastogi, N.; Sharma, D.; Singh, D. Inter and Intra-Annual Variability in Aerosol Characteristics over Northwestern Indo-Gangetic Plain. *Aerosol Air Qual. Res.* **2015**, *15*, 376–386. [[CrossRef](#)]
57. Wu, R.; Zhou, X.; Wang, L.; Wang, Z.; Zhou, Y.; Zhang, J.; Wang, W. PM<sub>2.5</sub> Characteristics in Qingdao and across Coastal Cities in China. *Atmosphere* **2017**, *8*, 77. [[CrossRef](#)]
58. Ye, Z.; Li, Q.; Liu, J.; Luo, S.; Zhou, Q.; Bi, C.; Ma, S.; Chen, Y.; Chen, H.; Li, L.; et al. Investigation of submicron aerosol characteristics in Changzhou, China: Composition, source, and comparison with co-collected PM<sub>2.5</sub>. *Chemosphere* **2017**, *183*, 176–185. [[CrossRef](#)] [[PubMed](#)]
59. Turpin, B.J.; Lim, H.J. Species contributions to PM<sub>2.5</sub> mass concentrations: Revisiting common assumptions for estimating organic mass. *Aerosol Sci. Technol.* **2001**, *35*, 602–610. [[CrossRef](#)]
60. Bernardoni, V.; Elser, M.; Valli, G.; Valentini, S.; Bigi, A.; Ferrero, P.; Piazzalunga, A.; Vecchi, R. Size-segregated aerosol in a hot-spot pollution urban area: Chemical composition and three-way source apportionment. *Environ. Pollut.* **2017**, *231*, 601–611. [[CrossRef](#)] [[PubMed](#)]
61. Pakkanen, T.A.; Kerminen, V.M.; Loukkola, K.; Hillamo, R.E.; Aarnio, P.; Koskentalo, T.; Maenhaut, W. Size distributions of mass and chemical components in street-level and rooftop PM<sub>1</sub> particles in Helsinki. *Atmos. Environ.* **2003**, *37*, 1673–1690. [[CrossRef](#)]
62. Agarwal, S.; Aggarwal, S.G.; Okuzawa, K.; Kawamura, K. Size distributions of dicarboxylic acids, ketoacids, alpha-dicarbonyls, sugars, WSOC, OC, EC and inorganic ions in atmospheric particles over Northern Japan: implication for long-range transport of Siberian biomass burning and East Asian polluted aerosols. *Atmos. Chem. Phys.* **2010**, *10*, 5839–5858. [[CrossRef](#)]
63. Budisulistiorini, S.H.; Baumann, K.; Edgerton, E.S.; Bairai, S.T.; Mueller, S.; Shaw, S.L.; Knipping, E.M.; Gold, A.; Surratt, J.D. Seasonal characterization of submicron aerosol chemical composition and organic aerosol sources in the southeastern United States: Atlanta, Georgia, and Look Rock, Tennessee. *Atmos. Chem. Phys.* **2016**, *16*, 5171–5189. [[CrossRef](#)]
64. Young, D.E.; Allan, J.D.; Williams, P.I.; Green, D.C.; Flynn, M.J.; Harrison, R.M.; Yin, J.; Gallagher, M.W.; Coe, H. Investigating the annual behaviour of submicron secondary inorganic and organic aerosols in London. *Atmos. Chem. Phys.* **2015**, *15*, 6351–6366. [[CrossRef](#)]

65. Xu, P.; Zhang, J.; Ji, D.; Liu, Z.; Tang, G.; Jiang, C.; Wang, Y. Characterization of submicron particles during autumn in Beijing, China. *J. Environ. Sci. (China)* **2018**, *63*, 16–27. [[CrossRef](#)] [[PubMed](#)]
66. The Website of National Meteorological Information Center. Available online: <http://data.cma.cn/site/index.html> (accessed on 6 August 2018).
67. Ye, X.N.; Chen, J.M. Haze and particulate matter moisture absorption increased. *Chin. J. Nat.* **2013**, *35*, 337–341.
68. Tan, H.; Cai, M.; Fan, Q.; Liu, L.; Li, F.; Chan, P.W.; Deng, X.; Wu, D. An analysis of aerosol liquid water content and related impact factors in Pearl River Delta. *Sci. Total Environ.* **2017**, *579*, 1822–1830. [[CrossRef](#)] [[PubMed](#)]
69. Zhou, M.; Chen, C.H.; Wang, H.L.; Lou, S.R.; Qiao, L.P.; Chen, Y.R.; Li, L.; Huang, C.H.; Chen, M.H. The variation characteristics of organic and element carbon during air pollution episodes in autumn in Shanghai, China. *Acta Sci. Circ.* **2013**, *33*, 181–188.
70. Zhou, M.; Chen, C.H.; Qiao, L.P.; Lou, S.R.; Wang, H.L.; Huang, H.Y.; Wang, Q.; Chen, M.H.; Chen, Y.R.; Li, L.; et al. The chemical characteristics of particulate matters in Shanghai during heavy air pollution episode in Central and Eastern China in January 2013. *Acta Sci. Circ.* **2013**, *33*, 3118–3126.
71. Zhang, X.; Zhang, Y.; Sun, J.; Yu, Y.; Canonaco, F.; Prevot, A.S.H.; Li, G. Chemical characterization of submicron aerosol particles during wintertime in a northwest city of China using an Aerodyne aerosol mass spectrometry. *Environ. Pollut.* **2017**, *222*, 567–582. [[CrossRef](#)] [[PubMed](#)]
72. Ge, X.; He, Y.; Sun, Y.; Xu, J.; Wang, J.; Shen, Y.; Chen, M. Characteristics and Formation Mechanisms of Fine Particulate Nitrate in Typical Urban Areas in China. *Atmosphere* **2017**, *8*, 62. [[CrossRef](#)]
73. National Bureau of Statistics of China Energy Statistics Division. *China Energy Statistical Yearbook*; China Statistics Press: Beijing, China, 2016.
74. Larese, C.; Galisteo, F.C.; Granados, M.L.; Mariscal, R.; Fierro, J.L.G.; Furio, M.; Ruiz, R.F. Deactivation of real three way catalysts by CePO<sub>4</sub> formation. *Appl. Catal. B Environ.* **2003**, *40*, 305–317. [[CrossRef](#)]
75. Pant, P.; Harrison, R.M. Estimation of the contribution of road traffic emissions to particulate matter concentrations from field measurements: A review. *Atmos. Environ.* **2013**, *77*, 78–97. [[CrossRef](#)]
76. Myung, C.L.; Park, S. Exhaust nanoparticle emissions from internal combustion engines: A review. *Int. J. Automot. Technol.* **2012**, *13*, 9–22. [[CrossRef](#)]
77. Chen, P.; Wang, T.; Dong, M.; Kasoar, M.; Han, Y.; Xie, M.; Li, S.; Zhuang, B.; Li, M.; Huang, T. Characterization of major natural and anthropogenic source profiles for size-fractionated PM in Yangtze River Delta. *Sci. Total Environ.* **2017**, *598*, 135–145. [[CrossRef](#)] [[PubMed](#)]
78. You, S.; Yao, Z.; Dai, Y.; Wang, C.H. A comparison of PM exposure related to emission hotspots in a hot and humid urban environment: Concentrations, compositions, respiratory deposition, and potential health risks. *Sci. Total Environ.* **2017**, *599*, 464–473. [[CrossRef](#)] [[PubMed](#)]
79. Cui, X.; Luan, W.; Song, Z.; Ma, Y. A study of the spatial distribution and source of heavy metals in urban soil in Shijiazhuang City. *Geol. Chin.* **2016**, *43*, 683–690.
80. Lyu, Y.; Liu, L.; Guo, L.; Yang, Y.; Qu, Z.; Hu, X.; Zhang, G. Deposited atmospheric dust as influenced by anthropogenic emissions in northern China. *Environ. Monit. Assess.* **2017**, *189*. [[CrossRef](#)] [[PubMed](#)]
81. Wang, L.T.; Wei, Z.; Yang, J.; Zhang, Y.; Zhang, F.F.; Su, J.; Meng, C.C.; Zhang, Q. The 2013 severe haze over southern Hebei, China: Model evaluation, source apportionment, and policy implications. *Atmos. Chem. Phys.* **2014**, *14*, 3151–3173. [[CrossRef](#)]
82. Behrooz, R.D.; Esmaili-Sari, A.; Bahramifar, N.; Kaskaoutis, D.G.; Saeb, K.; Rajaei, F. Trace-element concentrations and water-soluble ions in size-segregated dust-borne and soil samples in Sistan, southeast Iran. *Aeolian Res.* **2017**, *25*, 87–105. [[CrossRef](#)]
83. Huang, X.; Liu, Z.; Liu, J.; Hu, B.; Wen, T.; Tang, G.; Zhang, J.; Wu, F.; Ji, D.; Wang, L.; et al. Chemical characterization and source identification of PM<sub>2.5</sub> at multiple sites in the Beijing-Tianjin-Hebei region, China. *Atmos. Chem. Phys.* **2017**, *17*, 12941–12962. [[CrossRef](#)]
84. The Official Website of Hebei Provincial Department of Environmental Protection. Available online: <http://www.hebhb.gov.cn/> (accessed on 6 August 2018).
85. Liu, B.S.; Cheng, Y.; Zhou, M.; Liang, D.N.; Dai, Q.L.; Wang, L.; Jin, W.; Zhang, L.Z.; Ren, Y.B.; Zhou, J.B.; et al. Effectiveness evaluation of temporary emission control action in 2016 winter in Shijiazhuang, China. *Atmos. Chem. Phys.* **2018**, *18*, 7019–7039. [[CrossRef](#)]

86. Shen, Z.; Cao, J.; Arimoto, R.; Han, Y.; Zhu, C.; Tian, J.; Liu, S. Chemical Characteristics of Fine Particles (PM<sub>1</sub>) from Xi'an, China. *Aerosol Sci. Technol.* **2010**, *44*, 461–472. [[CrossRef](#)]
87. Guo, J.L. Study of Chemical Composition Features and Sources Apportionment of Atmospheric Particulate Matter during Haze in Shijiazhuang. Master Thesis, Beijing University of Chemical Technology, Beijing China, 2015.
88. National Bureau of Statistics of China Industrial Statistics. *China Industry Statistical Yearbook*; China Statistics Press: Beijing, China, 2016.
89. The Official Website of Tianjin Municipal People's Government. Available online: <http://www.tj.gov.cn/> (accessed on 6 August 2018).
90. The Official Website of Tangshan Municipal People's Government. Available online: <http://www.tangshan.gov.cn/> (accessed on 6 August 2018).
91. Wang, L.; Wei, Z.; Wei, W.; Fu, J.S.; Meng, C.; Ma, S. Source apportionment of PM<sub>2.5</sub> in top polluted cities in Hebei, China using the CMAQ model. *Atmos. Environ.* **2015**, *122*, 723–736. [[CrossRef](#)]
92. The Official Website of Ministry of Ecology and Environment of the People's Republic of China. Available online: <http://www.zhb.gov.cn/> (accessed on 6 August 2018).



© 2018 by the authors. Licensee MDPI, Basel, Switzerland. This article is an open access article distributed under the terms and conditions of the Creative Commons Attribution (CC BY) license (<http://creativecommons.org/licenses/by/4.0/>).